

Influence of topography on the asymmetry of rill cross-section: A case in the Yuanmou dry-hot valley

Xingli Gu

China West Normal University

Jun Luo (✉ luojunxm@126.com)

China West Normal University

Bin Zhang

China West Normal University

Lei Wang

China West Normal University

Qiangjianzhong Wu

China West Normal University

Research Article

Keywords:

Posted Date: January 18th, 2022

DOI: <https://doi.org/10.21203/rs.3.rs-1244680/v1>

License:   This work is licensed under a Creative Commons Attribution 4.0 International License.

[Read Full License](#)

Abstract

Rill erosion is one of the most common modes of erosion, and the development conditions of the cross-sections asymmetric characteristics are still uncertain. To study the relationship between rill topography and rill cross-sectional asymmetry, we used the measuring needle board method to measure 712 groups of rill cross-section in the Yuanmou dry-hot valley area. Using correlation analysis and principal component analysis to investigate the topographical conditions of rill development, the results show that: (1) Asymmetry is main feature in rill cross-sections, and 53% of rill cross-sections are right-biased, and 47% of them are left-biased. (2) There is a significant positive correlation between the slope difference and the rill cross-section asymmetry ratio ($P < 0.01$). The asymmetry ratio increases as the slope difference on both sides (B) increases, and the directionality of the asymmetry ratio is affected by B . The difference between the catchment areas on both sides has a significant linear correlation with the asymmetry ratio of width ($r = 0.07$, $P < 0.05$). (3) 7 topographic factors are divided into two types of principal components: The first represents the rill slope surface shape and rill shape, including the rill length, rill slope length, rill head catchment area, and the four rill bending coefficient factors; the second principal component represents the difference between the two sides of the rill, including the difference in slope from side to side, the difference between the catchment areas on both sides and the location of turning angle of the rill.

Introduction

Soil erosion is one of the main environmental problems affecting humans, and causes about 5 to 7 million hectares of farmland loss every year¹. Gully erosion is one of the most important soil erosion processes and results in a soil loss rate of around 85%. Channel erosion includes rill erosion, ephemeral gully erosion, and gully erosion^{2,3}. Rill erosion is one of the initial forms of channel erosion⁴, usually eventually forming a gully⁵. Research on rill mainly focuses on the origin of rill cross-sectional morphology⁶, describing the relationship between general rill cross-sectional morphology and rill erosion⁷⁻¹⁰. Rill morphological characteristics form the basis for understanding the underlying mechanisms of the evolution of rill, and are important for estimating the rill erosion volume and rill erosion rate. Therefore, it is paramount to study the morphological characteristics of rill erosion.

Rill morphology includes planar, cross-sectional, and longitudinal morphology, and the cross-section is the most important morphological feature reflecting development stage of rill¹¹. In the early stage of rill development, the rill cross-section generally presents a "V" shape¹². With the continuous evolution of a rill, a "U" or "box" cross-section gradually appears, but the rill is still dominated by a "V"-shape cross-section^{13,14}. The morphological characteristics of the rill cross-section constitute its length¹⁵, depth¹⁵, width¹⁶, and asymmetry ratio¹⁷, and these characteristics change with the evolution of the rill¹². The length of a rill has a significant positive correlation with the evolution rate of its morphology, and its width and depth increase with length¹⁶. However, an increase in rill length and width leads to an increase in runoff and rill depth, and rill erosion becomes increasingly intense, which accelerates rill development

^{15,18}. The cross-sectional area of a rill is positively correlated with the rill catchment area. The greater the flow of water into a ditch, the more serious is rill erosion, and the larger the rill cross-sectional area ¹⁹. Asymmetry in a cross-section is the main feature in the erosion of gullies, and it is an extremely important parameter used to describe the morphological and dynamic characteristics of a watershed ^{20,21}. Cross-sectional asymmetry was first used to evaluate the morphologies of river beds, and was subsequently used to describe the cross-sectional morphologies of channels ^{20,22}. However, systematic quantification of rill asymmetry is still lacking.

Cross-sectional asymmetry is the result of several combined factors, such as bedrock ²³⁻²⁵, climate ²⁶, vegetation ^{27,28}, and topography. With regard to bedrock, studies in loess areas have found that the slope of a cross-section is steeper on the exposed side of the bedrock, and gentler on the side covered by the loess layer. This is because eroding the bedrock becomes more difficult than eroding loess deposits²⁴. With regard to climate, the sunward side is easily corroded by glacial melt runoff and expands to the rear side to form an asymmetric channel. This is because when the solar incident angle is large at noon and afternoon, the temperature of the sunward side groove wall increases, and it becomes more susceptible to erosion ²⁶. With regard to vegetation, a slope with good vegetation development has relatively low levels of runoff and erosion; a slope with poor vegetation development, or bare patches, has relatively high levels of runoff and erosion. The varying levels of runoff and erosion are integral in forming an asymmetrical channel cross-section ^{27,28}. With regard to topography, differences in topographic factors, such as slope ²⁹, slope length ²⁹, gully depth³⁰, and catchment area, all affect the evolution of asymmetrical cross-sections. However, currently, scholars believe that topography affects small regional climates and vegetation conditions indirectly, creating channel cross-sectional asymmetry. Most studies concentrate on large-scale channels such as gullies, and there are few studies on the rill cross-sectional asymmetry ratio (RCA) ^{23,24,27,31}.

Although there have been several studies on rill cross-sectional asymmetry, the influence of cross-sectional asymmetry on rill erosion, and the causes of cross-sectional asymmetry. However, quantitative research on the asymmetry characteristics of rill cross-sections is still lacking, and how topographic factors affect rill cross-sectional asymmetry remains to be resolved. The objectives of this study are: (1) To establish a rill cross-sectional asymmetric morphology index that describes the rill's cross-sectional shape, and permits the selection of key topographic factors; (2) to analyze the relationship between rill cross-sectional asymmetry and rill topographic factors. This reveals the evolutionary laws and mechanisms underlying rill morphology, and provides a reference for ecological restoration and soil erosion management.

Results

Statistical characteristics of the RCA

The RCA is a key parameter in describing rill morphology. It reflects the differences in certain aspects of natural conditions, resulting in inconsistent in development speeds on both sides of a rill cross-section. The results of this study show that asymmetry is widespread in the cross-section of a rill (Fig. 1). The A_w ranged from -1.77 to 1.97, with an average value of -0.034. There were 374 cross-sections whose RCA was less than or equal to 0, meaning 53% of the cross-sections were right-skewed. The A_a ranged from -1.81 to 1.71, with an average of -0.046. There were 374 cross-sections with an RCA of less than or equal to 0, meaning 53% of the cross-sections were right-skewed.

Figure 2 shows that there are four A_w groups in the interval (-1.7, -1.5), 53 groups in the interval (-1.5, -1.0), 144 groups in the interval (-1.0, -0.5), 173 groups in the interval (-0.5, 0), 174 groups in the interval (0, 0.5), 120 groups in the interval (0.5, 1.0), 39 groups in the interval (1.0, 1.5), and 5 groups in the interval (1.5, 2). The A_a has 15 groups in the interval (-1.8, -1.5), 63 groups in the interval (-1.5, -1.0), 130 groups in the interval (-1.0, -0.5), 166 groups in the interval (-0.5, 0), 161 groups in the interval (0, 0.5), 110 groups in the interval (0.5, 1.0), 53 groups in the interval (1.0, 1.5), and 14 groups in the interval (1.5, 2). The RCA of most cross-sections are concentrated in the interval (-0.5, 0.5). There are 588 cross sections in this interval, accounting for 82.6% of the total. This indicates that, although the rill cross-section has asymmetry, the difference between both sides of the section is weak (Fig. 5). This may be because of the small scale of rill and small variations in natural conditions, such as topography, on both sides of the section.

The influence of a single topographic factor on the RCA

Correlation analysis of the A_w , A_a , and the B, L, I, A, R, K, J was carried out. The results show that the main factors that have a significant linear correlation with the A_w and the A_a are B ($P < 0.01$), with correlation coefficients 0.32 and 0.22, respectively (Figure 3). That is, the greater the difference in slope between the two sides, the more asymmetric the rill cross-section. R also has a significant linear correlation with the A_w ($P < 0.05$), with a correlation coefficient of 0.07. This means the greater the difference in catchment between the left and right sides of the rill, the greater the asymmetry of the rill cross-section. However, other topographic factors have no significant correlation with the RCA. This is because these topographic factors have a significant correlation among themselves. They jointly affect the RCA, thus showing a high degree of correlation.

B is the the difference in slope between both sides of the catchment area to the rill cross-section. The smaller the difference in slope between the catchment areas on both sides, the closer B is to 0. When the catchment area slope on the right side of the cross section is greater than that on the left side, $B < 0$; and when the catchment area slope on the left side of the cross section is greater than that on the right side, $B > 0$. By grouping B, it is found that the average RCA increases as B increases (Figure 4). When B is (-30, -20], A_w is -0.48 and A_a is -0.38; when B is (-20, -10], A_w is -0.36 and A_a is -0.31; when B is (-10, 0), A_w is -0.23 and A_a is -0.22; when B is (0, 10], A_w is 0.21 and A_a is 0.16; when B is (10, 20), A_w is 0.47 and A_a is 0.40; when B is (20, 40], A_w is 0.31 and A_a is 0.13, which are relatively low values, because this group has only two sets of cross-sections, which cannot represent the characteristics of interval B. The sign of the RCA is the same as the sign of B. The directionality of the RCA is significantly affected by B. When the

slope of the left catchment area is large, $RCA > 0$, and the rill cross-section appears to the leftwards; when the slope of the right catchment area is large, $RCA < 0$, and the cross section appears to the rightwards.

The influence of multiple topographic factors on the RCA

In order to explore the influence of multiple topographic factors on the RCA, principal component analysis (PCA) is used to extract the main-feature components of the topographic data. The PCA results show that the 9 topographic factors can be reflected by 2 principal components to 61.84% (characteristic value: $3.117+1.211=4.328$ variables) (Table 1). Therefore, the analysis of the first two principal components has been able to reflect most of the information of all the data.

Table 1
Calculation results of topographic factor PCA

| Component | 1 | 2 |
|---------------|--------|--------|
| Total | 3.117 | 1.211 |
| % of Variance | 44.534 | 17.303 |
| Cumulative % | 44.534 | 61.838 |
| B | -.238 | .689 |
| L | .885 | .163 |
| I | .811 | .241 |
| A | .875 | -.003 |
| R | -.587 | .557 |
| K | .602 | -.111 |
| J | .384 | .574 |

The contribution rate of the first principal component is 44.534%. The characteristic is that the factor variables have high positive loads for the four factors L, I, A, and K. L has the largest contribution rate, at 88.5%, followed by A, I, and K, at 87.5%, 81.1%, and 60.2%, respectively. Therefore, the first component represents rill slope and rill shape.

The contribution rate of the second principal component is 17.303%. The characteristic is that the factor variables have high positive loads for the three factors B, J, and R. B has the largest contribution rate, at 83.5%, followed by J and R, at 57.4% and 55.7%, respectively. Therefore, the second component represents the effect of the difference between the two sides of the rill.

Discussion

This study shows that the difference in slope between the left and right sides has a significant positive correlation ($P < 0.01$) with the A_w and the A_a ; and the difference in rill catchment area between both sides has a significant linear correlation ($P < 0.05$) with the A_w . Other single topographic factors have no significant correlation with the RCA. Regarding the influence of multiple topographical factors on rill cross-sectional asymmetry, the first principal component represents the rill slope and rill shape, including L, I, A, and K. The second component represents the effect of the difference between the two sides of the rill, including B, J and R.

In addition to being affected by topographical factors, the cross-sectional shape of the rill is affected by factors such as rainfall, vegetation, soil, runoff, slope characteristics, and human activity. Rainfall splashing vertically on the slope will cause rill erosion there³². The degree of rill erosion varies with the intensity of rainfall³³. After rainfall produces runoff on the slope, it erodes the rill slope. The greater the runoff on the slope, the greater the amount of rill erosion³⁴. The degree of surface vegetation coverage is an important indicator that determines the erosion resistance of slope rills. It can reduce the direct impact of rainfall on the surface, and it can reduce the intensity of runoff erosion³⁵. Soil erosion resistance is also a main factor affecting rill erosion, Soils with a greater clay content appear to form narrower and deeper rills for a given erosive force³⁶. The evolution of rill cross-sections³⁶ is not only affected by natural conditions, but by human activity. Both are important in shaping rill morphology and accelerating soil erosion³⁷. In areas with severe rill erosion, harmful farming practices exacerbate it, which, in turn, causes accelerated soil erosion on slopes. Therefore, human influence is also an important aspect that cannot be ignored.

The RCA of the 712 cross-sections was right-skewed cross-sections accounted for 53%. This means that most of the rill is shifting to the right (Figure 5). This is consistent with the results for the morphological characteristics of gully cross-sections in the Yuanmou dry-hot valley. Results have shown that of all the 456 cross-sections measured in the study area, 201 were right-deflection, 184 were left-deflection, and 71 were quasi-symmetrical¹⁷. Moreover, statistical results for loess gullies have shown that most watersheds shift towards the right of the geometric center line, thereby forming a specific asymmetrical gully morphology²⁴.

This study shows that the left-right bias of the RCA is consistent with B, and that B has a certain effect on the direction of the RCA. In the northern hemisphere, when water flows from upstream to downstream, it is deflected to the right under the action of the Coriolis force; this causes more serious erosion on the right side of a rill. However, the Coriolis force may be too small to directly affect the asymmetry of a cross-section¹⁷. However, many factors, such as rainfall, vegetation, soil properties, topography, and human activity, affect rill morphology²⁴. The influence of such factors on rill morphology requires further study, especially regarding what causes right deviation and left deviation from a channel cross-section.

Methods

Study area

Yuanmou County is located in the northern part of Yunnan Province (101°35'–102°06'E, 25°23'–26°06'N). On the eastern part of the province is situated Dongshan Mountain, with an altitude of more than 2500 m. The western part of Dongshan Mountain is a gentle slope. Most of the exposed rock layers in the area constitute metamorphic rocks, sandstones, mudstones, and mid-late Pleistocene terrace deposits. Fluvial and lacustrine sedimentary rocks are widely distributed. The climate in the study area is dry and hot, with an average annual temperature of 21.9°C, long periods of sunshine throughout the year, an average annual rainfall of 630 mm, and evaporation is about 6 times the amount of rainfall. The zonal soils constitute dry red soil, vertisol, and alluvial soils. The vertisol and the alluvial soils have very poor anti-erosion ability. In addition, the vegetation coverage on the surface is very low. When the rainy season (June to October) comes, the rainfall is considerable, which makes the soil erosion in this area extremely serious. This soil erosion greatly restricts local economic development and human safety. This study selects Shadi Village, Gantang, Tutujiliangzi, Yuanmouren Site, Julin, and Banzaoli Village as research area (Figure 6).

Data acquisition

One hundred and sixty-six rills were selected in the study area randomly. According to the different rill lengths, select 3-5 typical cross-sections at equal intervals for surveying and mapping, at the head, upper middle, lower middle and upper part of the groove respectively for surveying and mapping. A total of 712 cross-sections were acquired, and a measuring needle plate method was used to trace a selected rill cross-section (Figure 7). A dinometer was used to measure the slope of the trench wall on both sides of the trench at the location of the section. Rill slope was measured on both sides of the rill at the section's position. The length of the rill slope, the actual length of the rill, the straight line length of the rill, and the height difference of the rill developed slope surface were measured with a tape measure, and the catchment areas on the left and right sides of the section and the catchment area at the head of the rill were calculated. A compass was used to measure the overall direction of the rill and the direction of the upper and lower sections, and the turning angle of the rill at each section was calculated.

Methods

- Rill cross-sectional parameters

Data processing constitutes the following: Correct the measured cross-sectional data using a coordinate conversion formula, and then use AutoCAD2018 software to extract the cross-sectional morphological parameters. Measure the general morphological indicators of a rill cross-section: width (W), rill depth (D), actual rill length (L), asymmetry ratio of width (A_w), and asymmetry ratio of area (A_a)¹⁷. Details of rill cross-sectional parameters are shown in Figure 8 and Table 2.

Table 2
Cross-sectional parameters of a rill

| Parameter | | Definition, formula, and significance |
|-----------|--------------------------|--|
| Wr | Right width | Horizontal distance between the right vertex and the bottom |
| Wl | Left width | Horizontal distance between the left vertex and the bottom |
| Dr | Depth of right side | Vertical distance between the right-top and the bottom |
| Dl | Depth of left side | Vertical distance between the left-top and the bottom |
| Sr | Area of left side | Eroded area of left side |
| Sl | Area of right side | Eroded area of right side |
| S | Area of cross-section | $S = Sl + Sr$, to describe total eroded area |
| Aw | Asymmetry ratio of width | $A_w = (Wl - Wr) / [(Wl + Wr) / 2]$, to describe distance difference between right and left erosion |
| Aa | Asymmetry ratio of area | $A_a = (Sl - Sr) / [(Sl + Sr) / 2]$, to describe area difference between right and left erosion |

- Topographic factors parameters

Use Microsoft Excel to calculate the slope difference between the left and right sides of the rill wall, the length of the rill slope, the catchment area of the rill head, the difference between the left catchment area and the right catchment area, the bending coefficient of the rill, and the cross-sectional position turning angle. Details of the parameters of the topographic factors are shown in Table 3.

Table 3
Topographic parameters

| Parameter | | Definition, formula, and significance |
|-----------|--|---|
| Bl | Left-side slope | Slope of the catchment area to the left of the rill cross-section |
| Br | Right-side slope | Slope of the catchment area to the right of the rill cross-section |
| B | Slope difference on both sides | B= Bl-Br, describes the difference in slope between both sides of the catchment area to the rill cross-section |
| L | Rill length | Distance between the head of the rill to the tail of the rill |
| I | Rill slope length | Length of the slope where the rill is located |
| A | Rill head catchment area | |
| Rl | Catchment area on the left side of the section | Area enclosed from the left side of the section to below the trench head or the previous section |
| Rr | Catchment area on the right side of the section | Area enclosed from the right side of the section to below the trench head or the previous section |
| R | Difference between the catchment areas of both sides | R= Rl-Rr, describes the difference in catchment area between both sides of the rill section |
| K | Rill bending coefficient | Ratio of trench bottom curve length to trench bottom straight line length |
| J | Location of section angle of turning of rill | Difference between the inflow direction of the upper rill water and the outflow direction of the lower rill water at the section location |

Analysis

- Simple correlation analysis

Simple correlation analysis is a statistical analysis method used to study the correlation between two or more random variables for a given position. It can effectively indicate whether two variables change in the same direction or in the opposite direction. The simple correlation coefficient calculation formula is 38.

$$R_{xy} = \frac{\sum_{i=1}^n (x_i - \bar{x})(y_i - \bar{y})}{\sqrt{\sum_{i=1}^n (x_i - \bar{x})^2} \sqrt{\sum_{i=1}^n (y_i - \bar{y})^2}}$$

1

In formula (1), Rxy represents the simple linear correlation coefficient between x and y influencing factors, xi, yi represents the related parameters of the rill cross-sectional and topographic factors. The value range

of R_{xy} is $[-1, 1]$. When $R_{xy} < 0$, it means that there is a negative correlation between the two influencing factors, and when $R_{xy} > 0$, it means that there is a positive correlation.

- Principal component analysis

This literacy uses factor analysis to analyze the topographic factors and RCA with descriptive statistics in Statistical Package for Social Science (SPSS) Version 20 software. There was a strong correlation between topographic factors, and the concomitancy probability of Bartlett's Test of Sphericity was 0.000, less than the significance level of 0.05. Therefore, the data in this study were suitable for factor analysis (Table 4).

Table 4
KMO and Bartlett's Test

| | | |
|--|--------------------|-------------|
| Kaiser–Meyer–Olkin measure of sampling adequacy | | .644 |
| Bartlett's Test of Sphericity | Approx. Chi-Square | 349.530 |
| | df | 21 |
| | Sig. | 0.00X |

Declarations

Acknowledgements

This study was financially supported by National Natural Science Foundation of China (41971015) and Research Startup Project of China West Normal University (412732, 412745, 20E030)

Author contributions statement

Xingli Gu, Jun Luo, Bin Zhang, Lei Wang and Qiangjianzhong Wu conceived and designed the study. Jun Luo and Lei Wang collected the data. Xingli Gu analyzed the data. Xingli Gu wrote the paper. All authors read and approved the final manuscript.

References

1. Tang, K., Zhang, K. & Lei, A. Critical slope gradient for compulsory abandonment of farmland on the hilly Loess Plateau. *Chinese Science Bulletin* **43**, 409-412, doi:10.1007/bf02883721 (1998).
2. Kertész, Á. & Gergely, J. Gully erosion in Hungary, review and case study. *Procedia - Social and Behavioral Sciences* **19**, 693-701, doi:10.1016/j.sbspro.2011.05.187 (2011).
3. Poesen, J., Nachtergaele, J., Verstraeten, G. & Valentin, C. Gully erosion and environmental change: importance and research needs. *Catena* **50**, 91-133, doi:10.1016/s0341-8162(02)00143-1 (2003).

4. Wang, B. *et al.* Effects of Near Soil Surface Characteristics on Soil Detachment by Overland Flow in a Natural Succession Grassland. *Soil Science Society of America Journal* **78**, 589-597, doi:10.2136/sssaj2013.09.0392 (2014).
5. Parhizkar, M., Shabanpour, M., Zema, D. A. & Lucas-Borja, M. E. Rill Erosion and Soil Quality in Forest and Deforested Ecosystems with Different Morphological Characteristics. *Resources* **9**, 129, doi:10.3390/resources9110129 (2020).
6. Zegeye, A. D. *et al.* Morphological dynamics of gully systems in the subhumid Ethiopian Highlands: the Debre Mawi watershed. *Soil* **2**, 443-458, doi:10.5194/soil-2-443-2016 (2016).
7. Zheng, F.-l., Xiao, P.-q. & Gao, X.-t. Rill erosion process and rill flow hydraulic parameters. *International Journal of Sediment Research* **19**, 130-141, doi:CNKI:SUN:GJNS.0.2004-02-004 (2004).
8. Hao, H. X., Guo, Z. L., Zhao-Xia, L. I. & Hua, L. Characteristics of Rill Cross-Section Morphology and Hydrodynamics on Red Soil Slope. *Resources and Environment in the Yangtze Basin* (2018).
9. Cai, Q. G., Zhu, Y. D. & Wang, S. Y. Research on processes and factors of rill erosion. *Advances in Water ence* **15**, 12-18, doi:10.1300/J 064v24n01_09 (2004).
10. Wang, J., He, L. I., Meng, Q., Wang, Y. & Zhang, Q. Characteristics of Rill Cross Section Morphology, Hydrodynamics and Sediment-carrying Capacity on Loess Slopes. *Journal of Soil and Water Conservation* **29**, 6, doi:10.13870/j.cnki.stbcxb.2015.03.007 (2015).
11. Gao & P. *Rill and Gully Development Processes*. Vol. 7 122-131 (Elsevier, 2013).
12. Deng, Q. C. *et al.* Experimental investigations of the evolution of step-pools in rills with heterogeneous soils in Yuanmou Dry-Hot Valley, SW China. *Catena* **194**, 104690, doi:10.1016/j.catena.2020.104690 (2020).
13. Zhang, Y., Wu, Y., Liu, B., Zheng, Q. & Yin, J. Characteristics and factors controlling the development of ephemeral gullies in cultivated catchments of black soil region, Northeast China. *Soil and Tillage Research* **96**, 28-41, doi:10.1016/j.still.2007.02.010 (2007).
14. Gabet, E. J. & Bookter, A. A morphometric analysis of gullies scoured by post-fire progressively bulked debris flows in southwest Montana, USA. *Geomorphology* **96**, 298-309, doi:10.1016/j.geomorph.2007.03.016 (2008).
15. Liu, Q. J., An, J., Wang, L. Z., Wu, Y. Z. & Zhang, H. Y. Influence of ridge height, row grade, and field slope on soil erosion in contour ridging systems under seepage conditions. *Soil & Tillage Research* **147**, 50-59, doi:10.1016/j.still.2014.11.008 (2015).
16. Tian, P., Xu, X., Pan, C., Hsu, K. & Yang, T. Impacts of rainfall and inflow on rill formation and erosion processes on steep hillslopes. *Journal of Hydrology* **548** (2017).
17. Deng, Q. C. *et al.* Characterizing the morphology of gully cross-sections based on PCA: A case of Yuanmou Dry-Hot Valley. *Geomorphology* **228**, 703-713, doi:10.1016/j.geomorph.2014.10.032 (2015).
18. Han, P., Ni, J. R., Hou, K. B., Miao, C. Y. & Li, T. H. Numerical modeling of gravitational erosion in rill systems. *International Journal of Sediment Research* **26**, 403-415, doi:Doi 10.1016/S1001-6279(12)60001-8 (2011).

19. Wang, N. *et al.* Variation of rill cross-sections with gravel and aggregating soil in the Dry-Hot Valley (SW China). *Modeling Earth Systems and Environment* **5**, 1239-1252, doi:10.1007/s 40808-019-00632-9 (2019).
20. Knighton, A. D. Asymmetry of river channel cross-sections: Part II. mode of development and local variation. *Earth Surface Processes and Landforms* **7**, 117-131, doi:10.1002/esp.3290070206 (1982).
21. Leopold, L. B. & Wolman, M. G. River Meanders. *Geological Society of America Bulletin* **71**, 769, doi:10.1130/0016-7606(1960)71[769:rm]2.0.co;2 (1960).
22. Shen, H. W. & Komura, S. Meandering Tendencies in Straight Alluvial Channels. *Journal of the Hydraulics Division* **94**, 997-1016, doi:10.1061/jyceaaj.0001866 (1968).
23. Burnett, B. N., Meyer, G. A. & McFadden, L. D. Aspect-related microclimatic influences on slope forms and processes, northeastern Arizona. *Journal of Geophysical Research* **113**, doi:10.1029/2007jf000789 (2008).
24. Chen, S. M., Xiong, L. Y., Duan, J. Z. & Tang, G. A. Formation of asymmetrical loess gullies in the northeastern loess plateau of China. *Earth Surface Processes and Landforms* **46**, 758-774, doi:10.1002/esp.5062 (2021).
25. Dohrenwend, J. C. Systematic valley asymmetry in the central California Coast Ranges. *Geological Society of America Bulletin* **89**, 891, doi:10.1130/0016-7606(1978)89<891:svaitc>2.0.co;2 (1978).
26. ZHONG, J. h., NI, J. r., WU, K. y. & LI, L. Unusual Erosion Channels in Yellow River Delta: Features and Genesis. *Geological Journal of Colleges and Universities*, 462-469, doi:10.3969/j.issn.1006-7493.2000.03.013 (2000).
27. Istanbuluoglu, E., Yetemen, O., Vivoni, E. R., Gutiérrez-Jurado, H. A. & Bras, R. L. Eco-geomorphic implications of hillslope aspect: Inferences from analysis of landscape morphology in central New Mexico. *Geophysical Research Letters* **35**, doi:10.1029/2008gl034477 (2008).
28. Wilcox, B. P. & Allen, B. ECOHYDROLOGY OF A RESOURCE-CONSERVING SEMIARID WOODLAND: EFFECTS OF SCALE AND DISTURBANCE. *Ecological Monographs* **73**, 223-239, doi:10.1890/0012-9615(2003)073[0223:EOARSW]2.0.CO;2 (2003).
29. Richardson, P. W., Perron, J. T., Miller, S. R. & Kirchner, J. W. Modeling the Formation of Topographic Asymmetry by Aspect-Dependent Erosional Processes and Lateral Channel Migration. *Journal of Geophysical Research: Earth Surface* **125**, doi:10.1029/2019jf005377 (2020).
30. Mulder, T. *et al.* New insights into the morphology and sedimentary processes along the western slope of Great Bahama Bank. *Geology* **40**, 603-606, doi:10.1130/G32972.1 (2012).
31. Poulos, M. J., Pierce, J. L., Flores, A. N. & Benner, S. G. Hillslope asymmetry maps reveal widespread, multi-scale organization. *Geophysical Research Letters* **39**, n/a-n/a, doi:10.1029/2012gl051283 (2012).
32. He, J. J., Sun, L. Y., Gong, H. L. & Cai, Q. G. Laboratory Studies on the Influence of Rainfall Pattern on Rill Erosion and Its Runoff and Sediment Characteristics. *Land Degradation & Development* **28**, 1615-1625, doi:10.1002/ldr.2691 (2017).

33. Shen, H. O., Zheng, F. L., Wen, L. L., Lu, J. & Jiang, Y. L. An experimental study of rill erosion and morphology. *Geomorphology* **231**, 193-201, doi:10.1016/j.geomorph.2014.11.029 (2015).
34. Sun, L. Y., Fang, H. Y., Qi, D. L., Li, J. L. & Cai, Q. G. A review on rill erosion process and its influencing factors. *Chinese Geographical Science* **23**, 389-402, doi:10.1007/s11769-013-0612-y (2013).
35. Shen, H. O., Zheng, F. L., Wen, L. L., Han, Y. & Hu, W. Impacts of rainfall intensity and slope gradient on rill erosion processes at loessial hillslope. *Soil & Tillage Research* **155**, 429-436, doi:10.1016/j.still.2015.09.011 (2016).
36. Ou, X. J., Hu, Y. X., Li, X. W., Guo, S. L. & Liu, B. Y. Advancements and challenges in rill formation, morphology, measurement and modeling. *Catena* **196**, 104932, doi:10.1016/j.catena.2020.104932 (2021).
37. Sidorchuk, A. Dynamic and static models of gully erosion. *Catena* **37**, 401-414, doi:10.1016/s0341-8162(99)00029-6 (1999).
38. Xu, J. Mathematical methods in contemporary geography. *China Higher Education Press, Beijing* **224230** (2002).

Figures

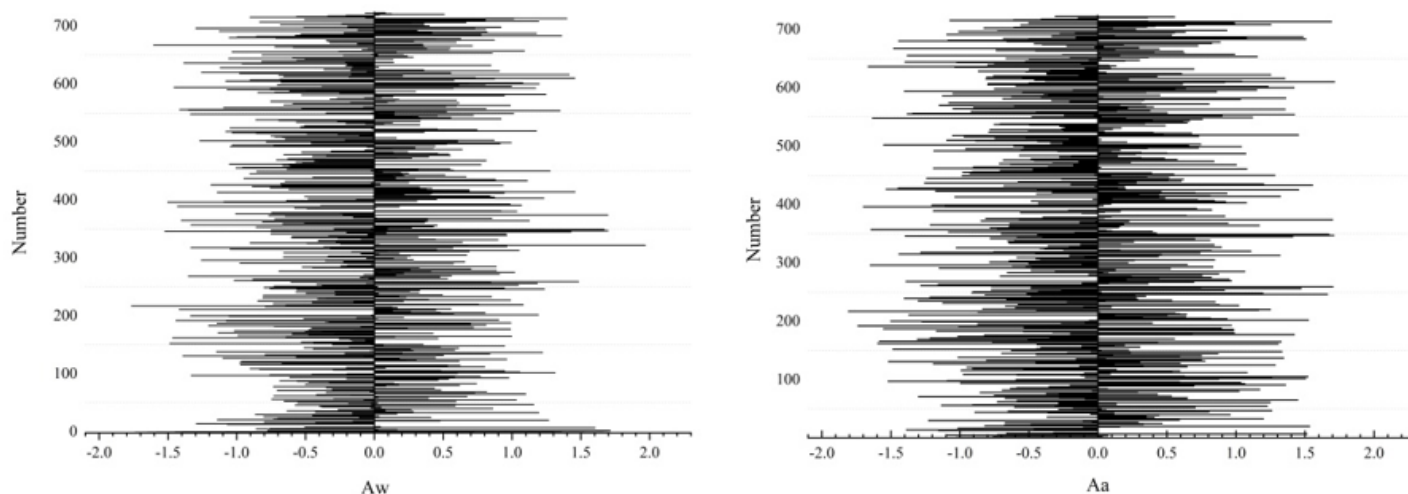
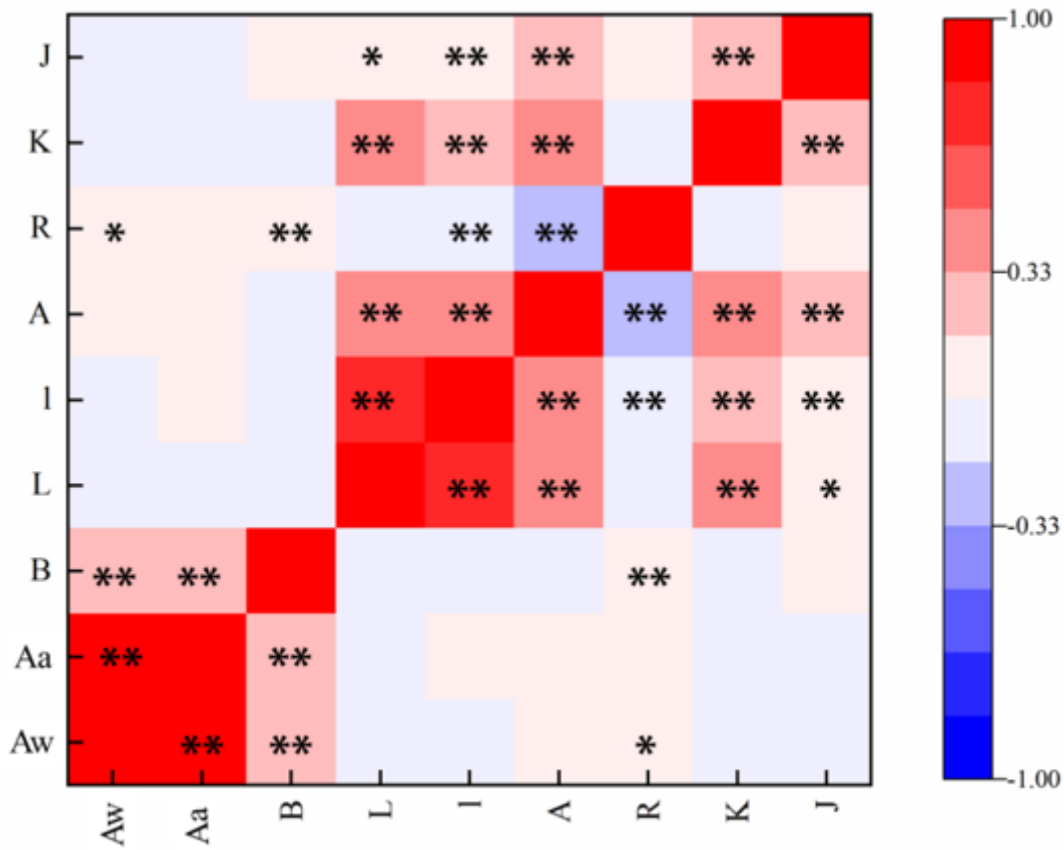


Figure 1

Statistical characteristics of the RCA

Figure 2

Distribution characteristics of the RCA



*: Correlation is significant at the 0.05 level (2-tailed).
 **: Correlation is significant at the 0.01 level (2-tailed).

Figure 3

Correlation between RCA and topographic factors

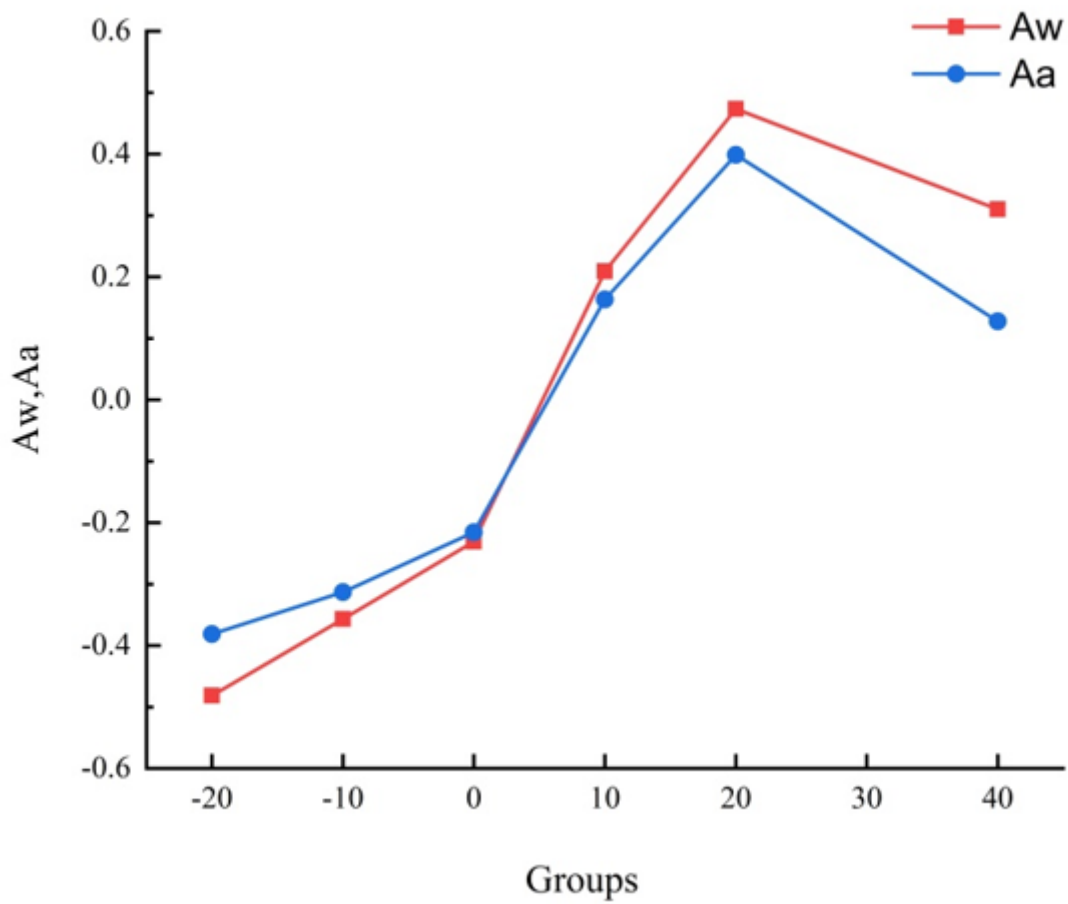


Figure 4

The asymmetry of different B values

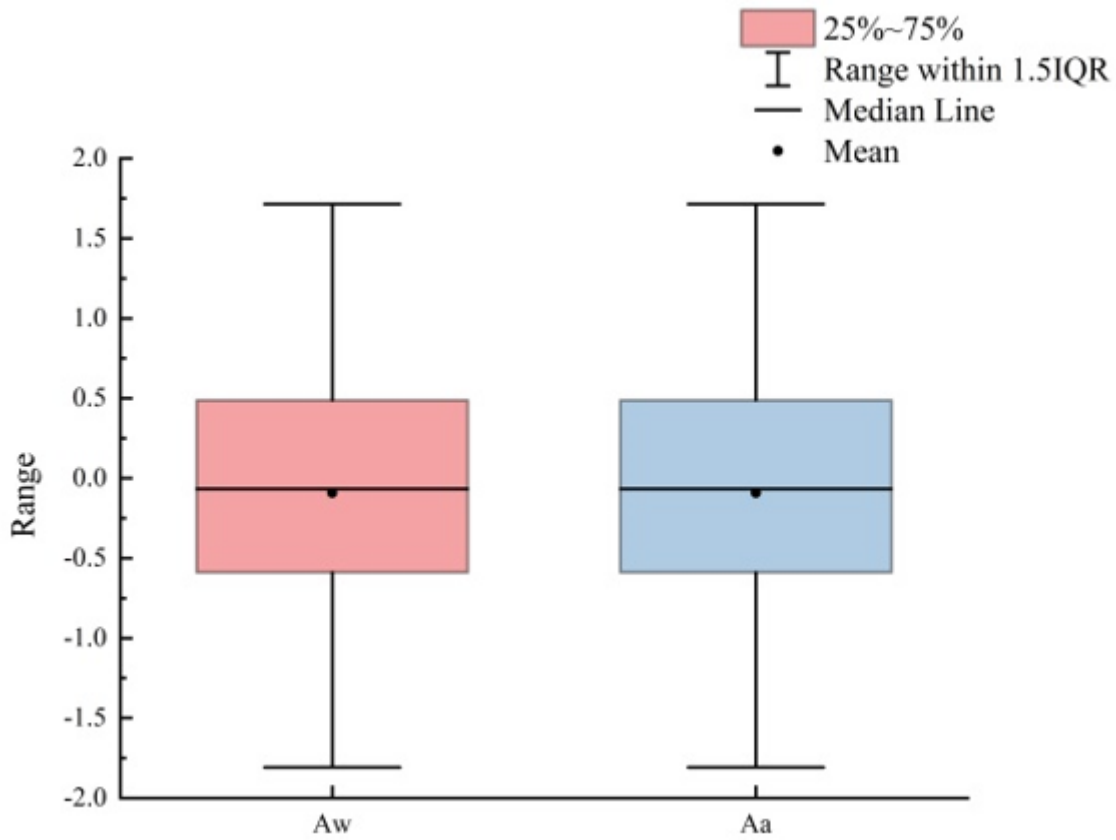


Figure 5

Directionality of the rill cross-section

Figure 6

Location of the study area

Figure 7

Schematic diagram of measurement

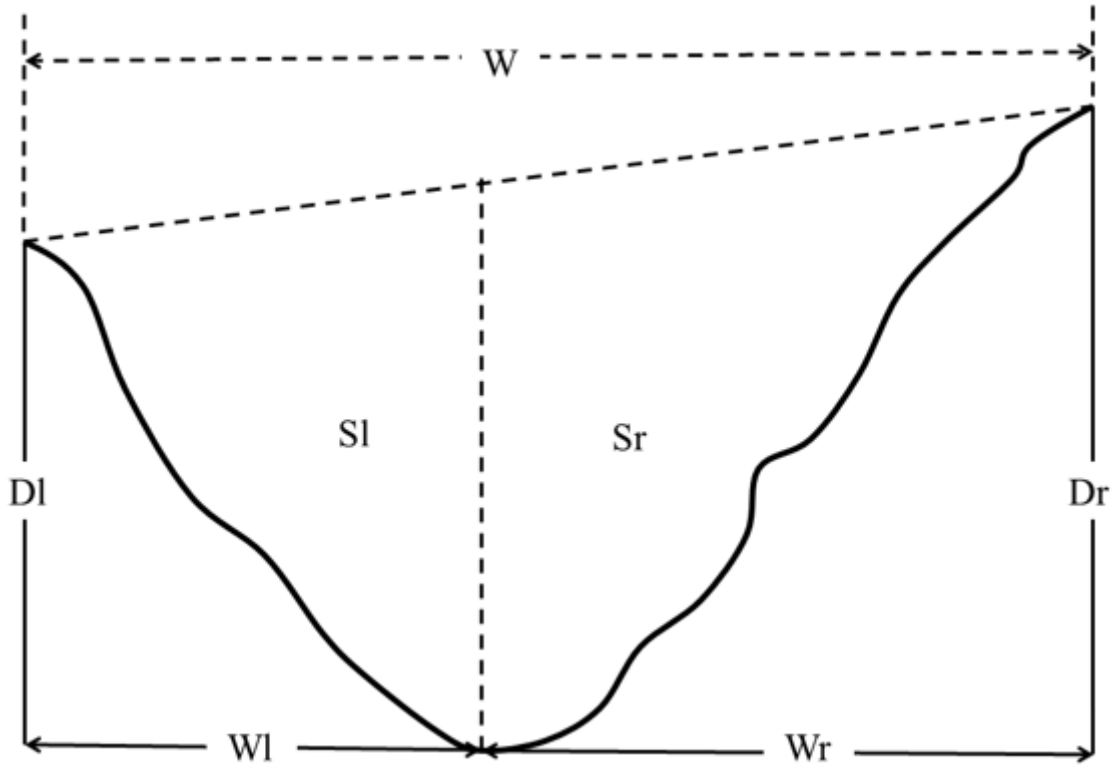


Figure 8

Schematic diagram of cross-sectional parameters